

Title page

Role of hypoxia in Diffuse Large B-cell Lymphoma: Metabolic repression and selective translation of HK2 facilitates development of DLBCL

Kavita Bhalla^{1,*}, Susan Jaber², Nanaji Nahid M³, Karen Underwood⁴, Afshin Beheshti⁵, Ari Landon⁶, Binny Bhandary¹, Paul Bastain⁷, Andrew M. Evens⁵, John Haley⁸, Brian Polster², and Ronald B. Gartenhaus^{1,3*}

¹Marlene and Stewart Greenebaum Comprehensive Cancer Center, University of Maryland, Department of Medicine, Baltimore MD 21201, USA; ²University of Maryland, Department of Biochemistry and Molecular Biology, Baltimore MD 21201, USA; ³Veterans Administration Medical Center, Baltimore, MD 21201, USA; ⁴University of Maryland, Flow Cytometry Core, Greenebaum Comprehensive Cancer Center, Baltimore MD 21201, USA; ⁵Tufts Medical Center, Boston, MA, 02111; ⁶Yale School of Medicine, Yale University, New Haven, CT, 06520; ⁷National Institute on Aging, National Institutes of Health, Baltimore, MD 21224, ⁸Department of Pathology, Stony Brook Medicine, Stony Brook, NY 11794-8691, USA.

Supplemental Material

Figure S1. Western blot analysis of mTORC targets in HLY and SUDHL2. HLY and SUDHL2 cells were grown for different time points at 1 % oxygen tension. Cells grown under normoxia were used as controls for the time points indicated in the figure. Protein lysates were obtained and expression levels of pMTOR, pRibosomalS6K, and p70S6K were determined using antibodies from Cell Signaling. GAPDH was used as an internal control for sample loading.

Figure S2. Microarray analysis of DLBCL cell lines HLY and SUDHL2. Co-correlation analysis of microarray data generated showed RNA enrichment of clinically relevant hypoxia metabolic targets in our dataset. Each column represents a sample for **(A)** HLY and **(B)** SUDHL2 cell lines that were cultured under normoxia and hypoxia, n=3. HLY and SUDHL2 cells were cultured in normal culture conditions and 1% hypoxia and microarray analysis was performed using Illumina gene chip. **(C)** Gene enrichment analysis of HIF1 α targets in the SUDHL2 dataset identified increased expression of glucose transporters SLC2A1 (GLUT1) and HK2 in hypoxia samples compared to those derived from normoxic cells. Top panel: heat map, bottom panel: fold change, *p<0.05, n=3, \pm SD. **(D)** List of ribosomal regulated genes.

Figure S3. Ingenuity Pathway (IPA) toxicity analyses. IPA toxicity analysis of microarray data in **(A)** HLY cell line, and **(C)** SUDHL2 cell line. Pathway analysis was filtered for pathways pertaining to mitochondria and hypoxia. Top mitochondrial pathways regulated under hypoxia are listed based on level of significance that are regulated under hypoxia are listed. X-axis is the $-\log$ of a p value and Y-axis represents different mitochondrial pathways regulated in DLBCL cell lines. (B and D) A detailed list of mitochondria-related genes that are regulated in respective mitochondrial pathways under hypoxia in HYL and SUDHL2 cell lines as determined by IPA toxicity analysis. (B, HLY) and (D, SUDHL2).

Figure S4. Expression of HIF1 α targets in normal B-cells derived from tonsils. Expression of HIF1 α targets was determined by RT-PCR analysis in primary B-cells derived from normal tonsils. There was no change in expression of glucose transporters in normal B-cells obtained from processing of tonsil tissue. However, the HIF1 α target VEGF was significantly induced under short-term hypoxic exposure of B cells compared to cells cultured under normoxia, $p < 0.05$, $n = 3$, \pm SD.

Figure S5. Measurement of ATP dependent OCR and immunofluorescence staining of mitochondrial markers in DLBCL cells. **(A)** ATP synthesis-dependent oxygen consumption rates of cells treated with hypoxia were unchanged relative to normoxia in DLBCL cell lines K422, HLY and Toledo. **(B)** HLY and Farage cells were also stained with MitoTracker green (MTG) to detect changes in mitochondrial mass. **(C and D)** Immunofluorescence staining of mitochondrial protein TOM20 and Cytochrome-C in DLBCL cells exposed to normoxia or hypoxia. There was intense staining of TOM20 and Cty-C in normoxic cells compared to cells cultured in 1% hypoxia.

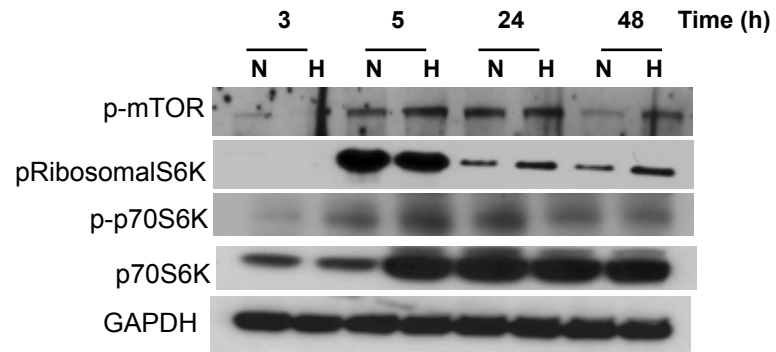
Figure S6. Growth characterization of DLBCL cells under hypoxic stress. **(A)** N=normoxia; H=hypoxia, $p < 0.05$, Flow cytometry data of cell cycle distribution are represented as a graph. For visualization purposes, each histogram is divided into three quadrants, each representing a G1/S/G2-M phase, as indicated in the figure. The percentage of cells accumulated in G2/M phase was significantly different from cells cultured in normoxia, $p < 0.05$. Results are expressed as $n = 3 \pm$ sd for A, B and C respectively. **(B and C)** Expression of markers indicative of cell cycle progression in HLY and SUDHL2 cells. Markers of mitotic induction (*CDC25B* and *CDC2*) were downregulated in SUDHL2 cells under hypoxic stress. In contrast, expression of *CDC25B* and *CDC2*, *CDC25A* were up-regulated in HLY cells when grown in 1% oxygen compared to normoxic control.

Figure S7. The presence of *eIF4E1* selectively stimulates expression of *HK2* under hypoxia. **(A)** Detection of *peIF4E1* and *eIF4E1* at indicated time points in HLY and SUDHL2 cells exposed to hypoxic stress. **(B and C)** Polysomal fractions were isolated from HLY and SUDHL2 cells cultured under normoxia and hypoxia and analyzed for *eIF4E1* and *HK2* levels by western blot analysis. **(D)** HLY cells were transfected with *eIF4E1* and selected with G418. Stably transfected cells were then subjected to normal culture conditions or hypoxic stress for 48 hrs. Protein lysates were obtained and expression of *HK2* was determined in the presence or absence of *eIF4E1*. **(E)** Luciferase assay using *HK2* promoter in COS7 cells to determine the effect of *eIF4E1* and *HIF1 α* on *HK2* promoter activity. COS7 cells transfected with *eIF4E1*, *HIF1 α* or both were incubated in 21% oxygen (normoxia) or 1 % oxygen (hypoxia) for 24 hrs and luciferase activity was measured using Promega dual activity luciferase kit. Renilla was used as an internal control.

Figure S8. Effect of *HK2* in promoting tumor growth. **(A and B)** RNA and protein expression of endogenous *HK2* levels in non-malignant B-cell line GM02184 (GM), primary B-cells derived from normal tonsil tissue (T1, T2) and DLBCL cell lines HLY, SUDHL2 and SUDHL6. **(C)** Knockdown of *HK2* levels in HLY using lentivirus (Origene). Cells expressed non-target shRNA (NT), shRNA *HK2* (Clones: sh5VA, sh5VB, sh5VC and sh5VD). shRNA clones sh5VA and sh5VB with efficient knock down were used for *in vitro* and *in vivo* growth experiments. **(D)** Xenograft tumors were established in NSG mice (n=5 per group, NT and sh*HK2*) using SUDHL2 cells expressing NT or sh*HK2* lentivirus. Growth of tumors was monitored for approximately 2 weeks and tumor volume was measured.

Figure S1

HLY



SUDHL2

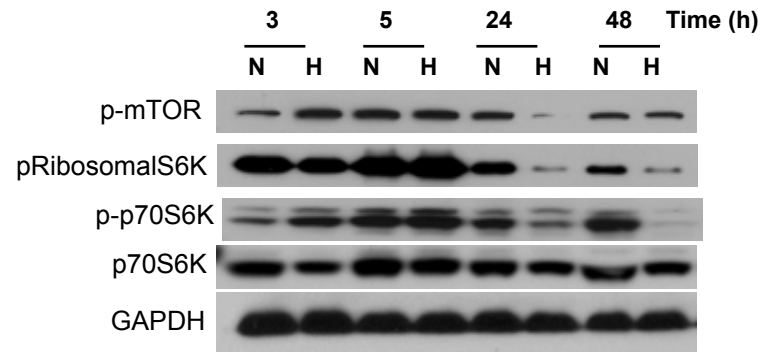


Figure S2

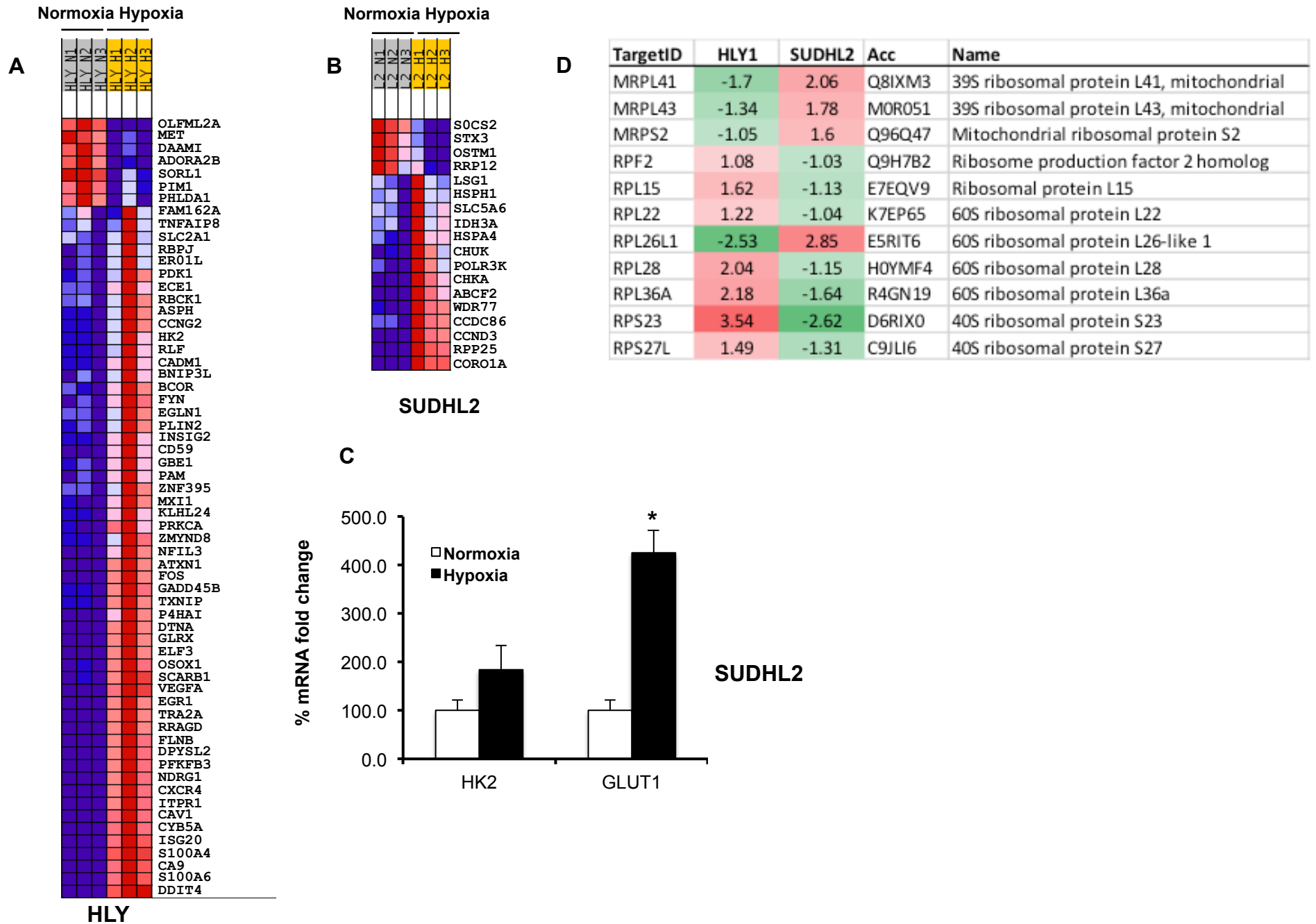
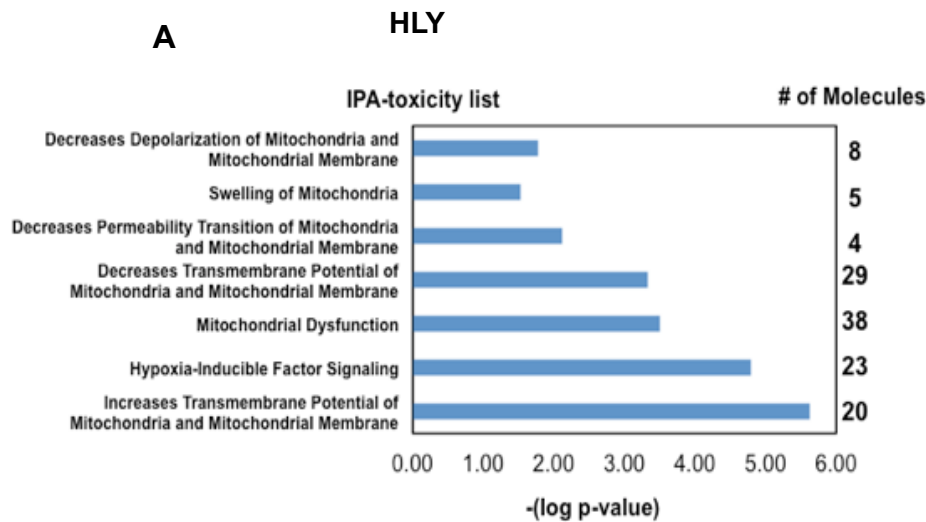
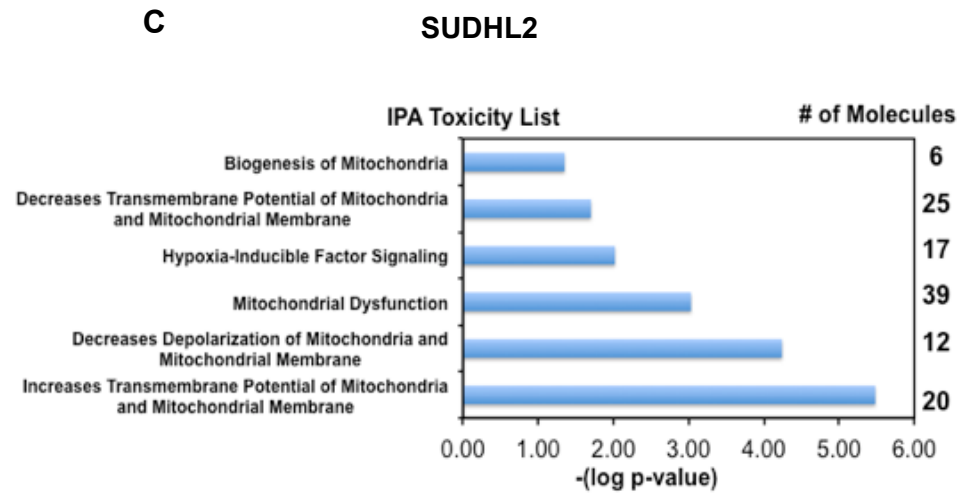


Figure S3



B HLY

Pathways	Molecules
Increase in transmembrane potential of MM	PTPN6,YWHAE,CASP3,RAC1,IL6,FAS,BCL2,HSPA4,SOD2,CD40,PIM1,HGF,CAT,CYCS,CFLAR,CD27,CASP7,PPARGC1A,LGALS1,TCL1A
Hypoxia inducible factor signaling	TP53,PIK3CA,EIF2B4,NQO1,MDM2,HIF1A,NOS3,UBE2L6,EIF2S2,EP300,VEGFA,PTK2,SHC1,UBE2J1,EIF1,UBE2H,CREB1,HIF1AN,EIF2B5,UBE2C,ATM,PRKCB,UBE2I
Mitochondrial dysfunction	FURIN,NDUFA7,ACO2,TRAK1,NCSTN,NDUFB8,PSEN2,ATP5S,SDHAP1,CYB5R3,BCL2,NDUFB9,SOD2,ATPAF1,GPX4,ACO1,OGDH,AIFM1,NDUFA8,SDHA,UCP2,CASP3,COX7A2L,NDUFB1,MAPK12,GPX7,GSR,FIS1,NDUFA6,UQCR10,CAT,UQCRC2,COX5A,APH1B,SDHD,CYCS,CYB5A,BACE2,COX15
Decrease in transmembrane potential of MM	CDKN2A,AATF,PYCARD,MUC1,MAPK13,FAS,DFFA,BCL2,MYC,SHC1,ZMAT3,SOD2,BID,IFI6,TP53,GZMA,UCP2,CASP3,AGA,PAWR,TCF3,ATPIF1,CAMP,SLC25A14,CASP2,PRKCD,CAT,RTN4,TNF,HSPB1
Decrease permeability transition of MM	BTG2,OGDH,HSPA5,BCL2
Swelling of mitochondria	TP53,TNF,FAS,BCL2,AIFM1
Decrease depolarization of mitochondria and Mitochondrial membrane	CAT,CDKN1A,PPIA,FAS,CSTB,MCL1,PPARGC1A,BCL2



D SUDHL2

Pathways	Molecules
Increase in transmembrane potential of MM	PTPN6,CASP3,ABL1,RAC1,FAS,BCL2,HSPA4,PRDX,SOD2,CD40,PHB,PIM1,HGF,CAT,CFLAR,CD27,CASP7,PPARGC1A,LGALS1,TCL1A
Decrease depolarization of MM	PAK1,CAT,CDKN1A,PPIA,PLIN3,MAP2K1,ATP2A2,FAS,CSTB,MCL1,PPARGC1A,BCL2
Mitochondrial dysfunction	FURIN,ATP5G1,ATP5D,NDUFA7,ACO2,TRAK1,NCSTN,NDUFB8,PSEN2,ATP5S,BCL2,NDUFB9,SOD2,ATPAF1,NDUFB6,GPX4,AIFM1,NDUFA8,ATP5G2,NDUFAF,UCP2,CASP3,GLRX2,NDUFB1,MAPK12,GPX7,GSR,FIS1,PRDX3,CAT,UQCRC2,COX5A,APH1B,SDHD,BACE2,CYB5A,NDUFS3,COX15
Hypoxia inducible factor signaling	EIF2B4,CSNK1D,PLCG1,MDM2,HIF1A,NOS3,UBE2L6,EIF2S2,EP300,UBE2D4,PTK2,JUN,UBE2J1,HIF1AN,EIF2B5,PRKCB,UBE2I
Decrease in transmembrane potential of MM	GZMA,CDKN2A,UCP2,CASP3,AATF,PYCARD,MUC1,AGA,MAPK13,TCF3,NFKB1,FAS,BCL2,FADD,DIABLO,SOD2,SLC25A14,PRKCD,CAT,RTN4,BCL2L2,BID,IFI6,TNF,HSPB1
Biogenesis of Mitochondria	PRDX3,GNAS,TFAM,SHARPIN,MAN2A1,PPARGC1A

Figure S4

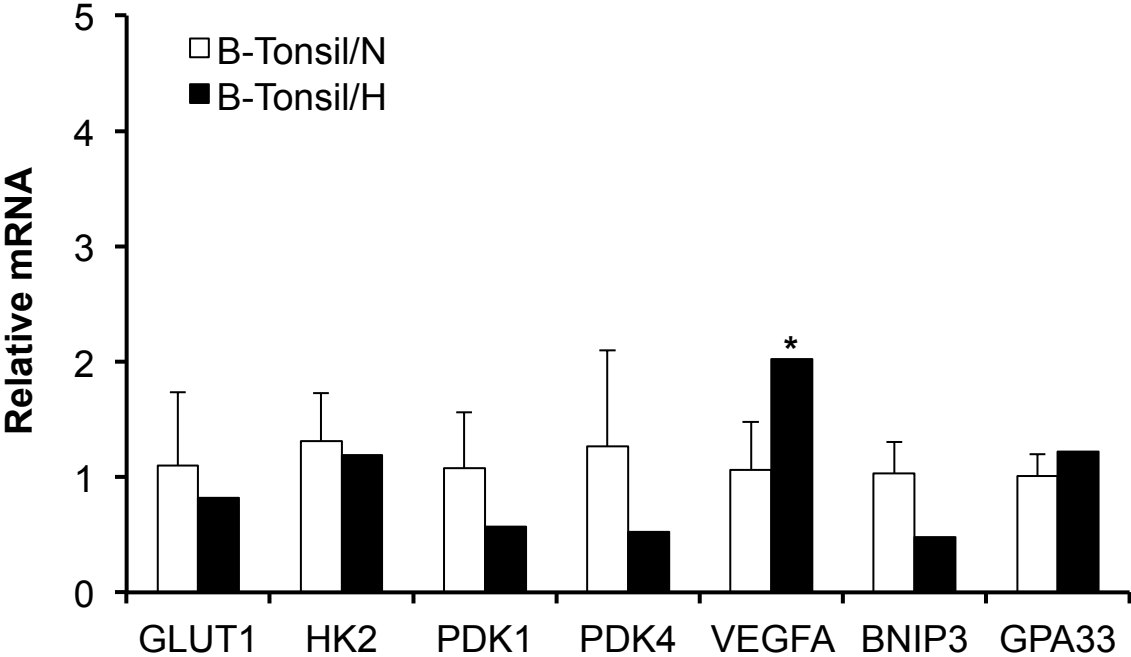


Figure S5

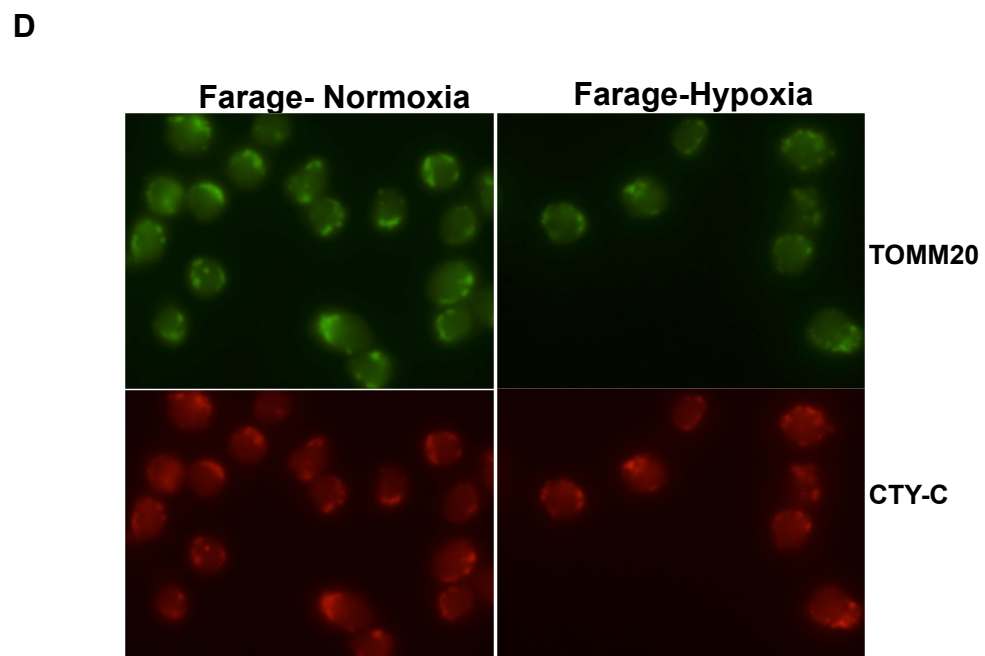
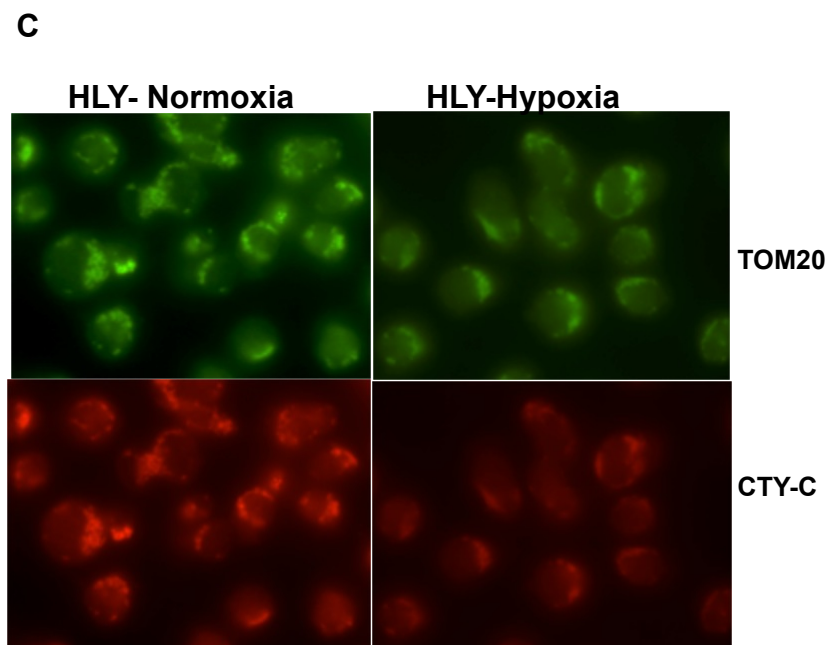
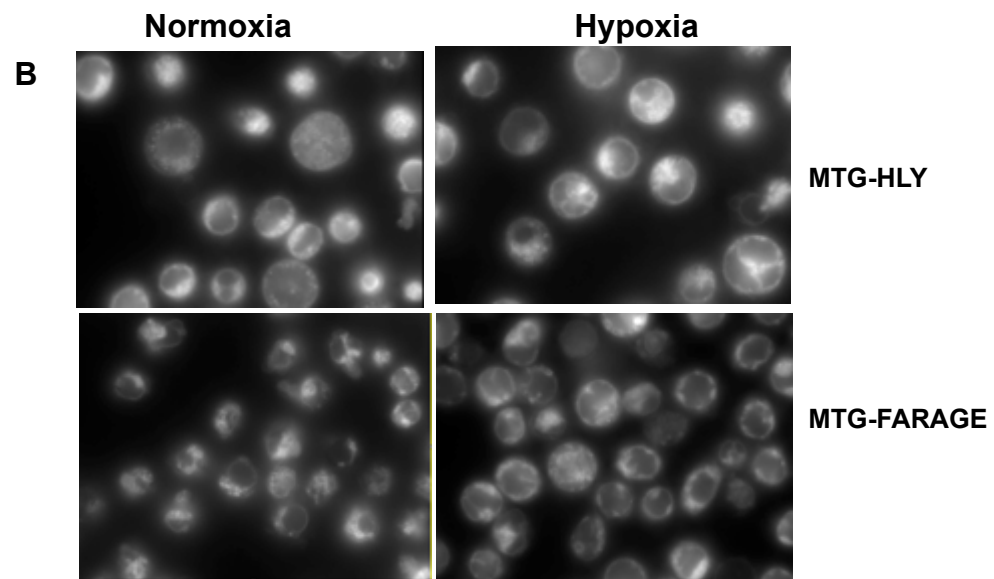
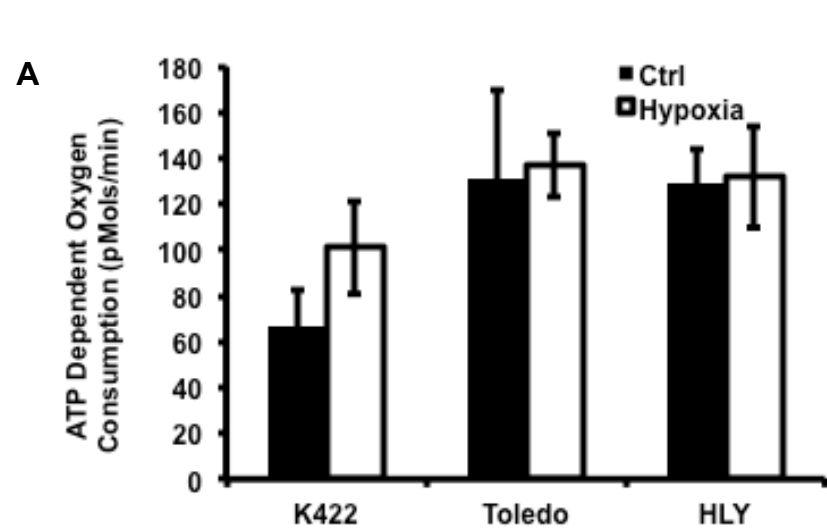


Figure S6

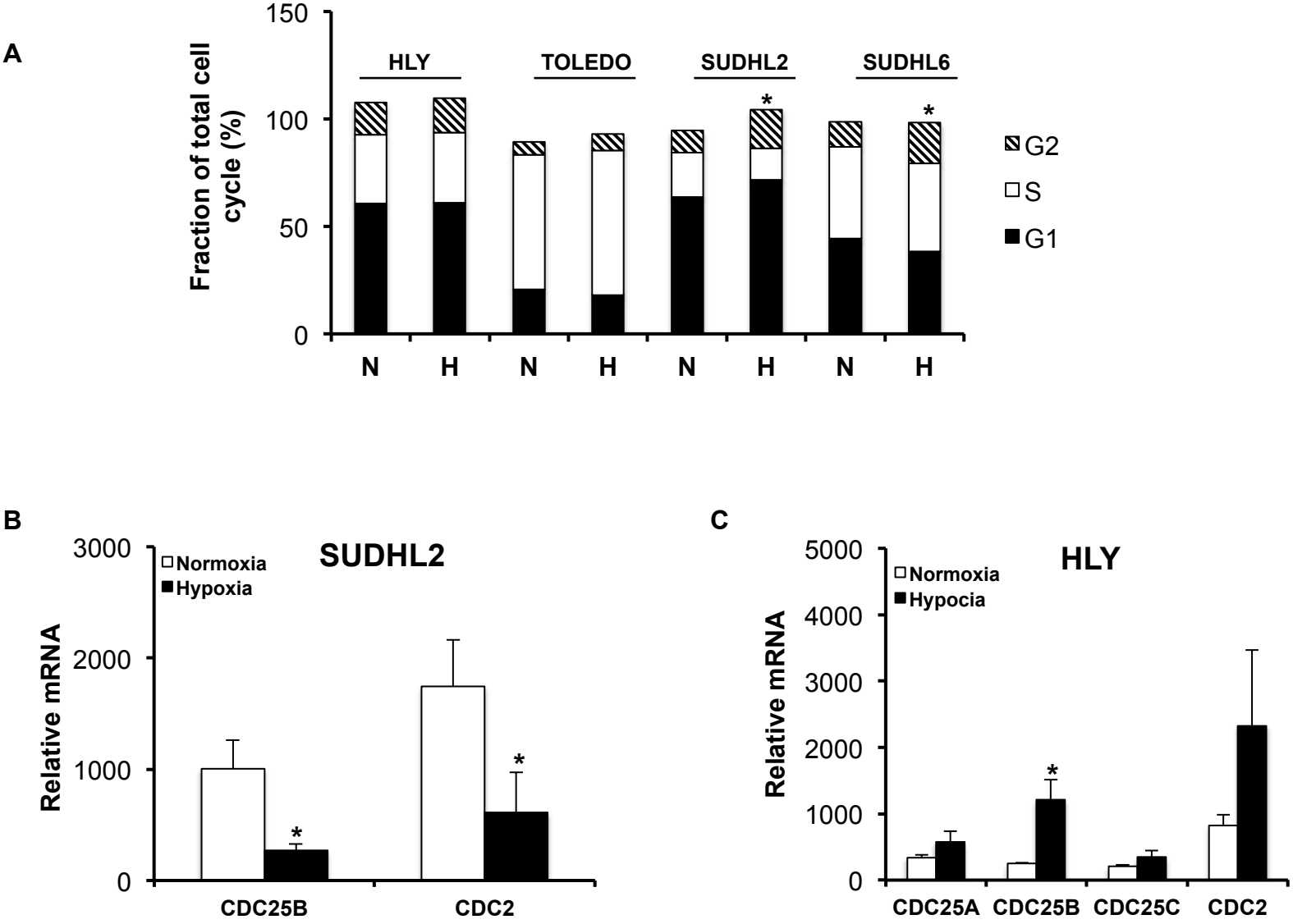


Figure S7

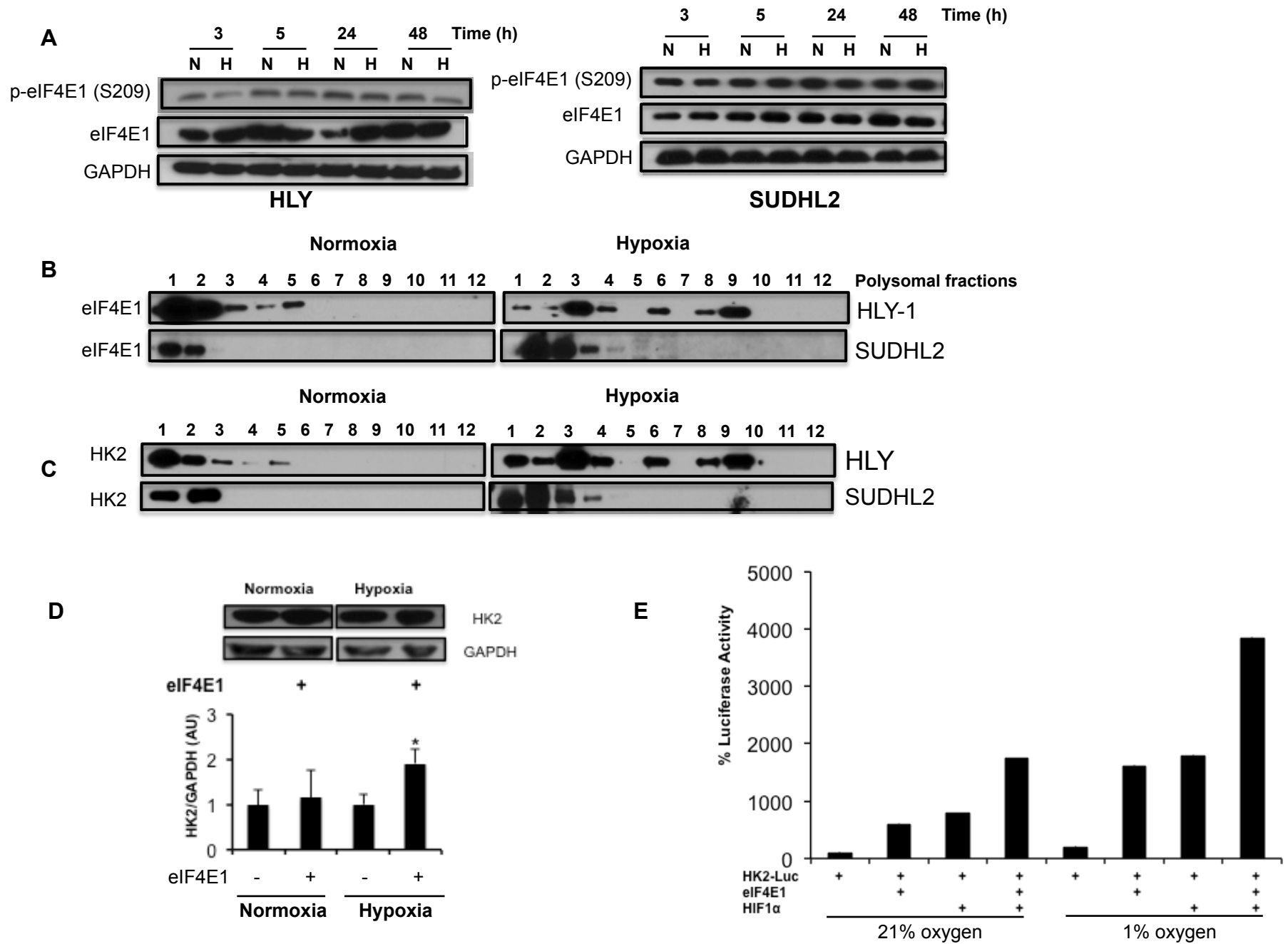


Figure S8

